JOURNAL OF CATALYSIS **115**, 319–325 (1989)

Acid Attack Theory of Dealumination in Cation-Exchanged Faujasite

JONG TAIK KIM,* MYUNG CHUL KIM,* YASUAKI OKAMOTO,† AND TOSHINOBU IMANAKA†

**Department of Industrial Chemistry, Kyungpook National University, Taegu 702-701, Korea; and*
†Department of Chemical Engineering, Faculty of Engineering Science, Osaka University,
Toyonaka, Osaka 560, Japan

Received January 7, 1988; revised August 8, 1988

The chemical extraction of Al atoms from X and Y zeolites during ion-exchange procedures using 1 *N* metal chloride solutions was experimentally and theoretically studied to reveal the effect of cation on the dealumination. The cation effect on the dealumination process was found to be related to the pH of the solution. Regardless of the cation, similar extents of dealumination were observed for the HCl solutions with the pH values equivalent to those of the metal chloride solutions. This suggests that the dealumination is initiated by an acid attack. CNDO/2 calculations were made on a six-ring model for a representative faujasite cluster to obtain atomic charge densities, Wiberg bond orders, and total energies. Total energy changes along reaction steps indicate a high possibility of the acid attack reaction mechanism.

INTRODUCTION

Dealumination of X and Y zeolites modifies strongly its catalytic activity. For instance, the acid strength of the zeolite increases as the aluminum content decreases (*1*). Dealuminated zeolites are prepared by the reaction of Na-zeolites with HCl (*2*), ethylenediaminetetraacetic acid (EDTA) (*3*), diethylenetriaminepentaacetic acid (DTPA), diaminocyclohexane *N,N,N′,N′*-tetraacetic acid(DCTA) (*4, 5*) and $SiCl_4$ (*6*). A reaction mechanism of the Al atom removal from zeolites was presented by Kerr (*3*). According to him, zeolite is changed, at least partially, to a hydrogen form before the removal of aluminum. The reaction involves hydrolysis of tetrahedral aluminum adjacent to a Brønsted acid site, followed by neutralization of the resultant basic aluminum hydroxide by protons to produce cationic aluminum species and water. However, the dealuminations which occur during conventional ion-exchanging procedures have not been fully studied.

Many workers (*7–9*) have tried theoretical studies to evaluate the cation–zeolite lattice interaction energy at each cation binding site. There are wide differences among their assumptions of cation ionicity. Recently, CNDO/2 calculations have been made on small clusters of faujasite six-ring for the sites S_{II} and $S_{I'}$ and of four-ring for the S_{III} site representing X and Y zeolites (*10*). In these cluster models, Al atoms are randomly arranged within the Loewenstein's rule. The distribution of Si and Al atoms in the faujasite framework has been confirmed by MAS NMR techniques (*11*).

Beran (*12*) studied qualitatively the effect of cation on the acidity of the skeletal and terminal hydroxyl groups by a CNDO/2 method. He used a hexagonal cluster model (*13*) with a $T_6O_6(OH)_{12}$ structure unit and theoretically evaluated the physicochemical characteristics of faujasite such as charge densities, bond orders, and electronic structures.

In the present study, the dealumination during a cation exchange was investigated. It was found that the extent of dealumination was determined by the proton concentration in the cation-exchanging solution. Theoretical calculations were made to rationalize these findings on the assumption of an acid attack mechanism.

0021-9517/89 $3.00

EXPERIMENTAL AND CALCULATION

The starting materials used in the preparation of cation-exchanged zeolites were Linde SK40 and 13X molecular sieves, whose compositions were $Na_{56}[(AlO_2)_{56}(SiO_2)_{136} \cdot 264H_2O$ and $Na_{86}[(AlO_2)_{86}(SiO_2)_{106} \cdot 276H_2O$, respectively. The dealumination of the faujasite-type zeolite was carried out at 100°C for 3 hr by a cation-exchange treatment with a 1 *N* cation chloride solution (2 *g* zeolite/30 ml solution). After the solution was drained, the sample was washed to assure its being free of chloride ion and dried under vacuum at room temperature. The powder obtained was stored over P_2O_5 in a desiccator.

The chemical analysis of the dealuminated samples was made on a Rigaku Model 3063P X-ray fluorescence spectrometer. The crystallinity of the zeolite was examined with a Jeol-88 X-ray diffractometer.

Pople's CNDO/2 method and a hexagonal cluster model (*13*) were used in calculations to simulate charge densities and Wiberg bond orders of Al–O and Si–O in the six-ring sites and the total energies of the zeolite clusters under consideration. The geometry of the cluster was taken from X-ray data (*14, 15*) and was adjusted for the different lengths of Si–O and Al–O bonds (0.161 and 0.175 nm (*16*), respectively). The open T–O bonds of the cluster were terminated by hydrogen atom in the direction of the next T in the framework. All the quantum-chemical calculations were accomplished taking into account only the orbitals lower in energy than 3*d* orbitals, i.e., the *sp* basis.

Convergence limits on the electronic energies were set equal to 1×10^{-6} a.u. The calculation provided results qualitatively identical with those of the calculations on the basis of the *spd* orbitals (*17, 18*). The CNDO/2 program and COORD program employed here were QCPE No. 261 and No. 226, respectively.

RESULTS AND DISCUSSION

Good crystallinities of the zeolites treated with 1 *N* alkali–metal chloride solutions were confirmed by X-ray diffraction. The peak heights in the X-ray diffraction patterns indicated partial destruction of the crystal structure of Fe^{2+}, Fe^{3+}, and H^+-zeolites. The decrease in the crystallinity of the zeolite was more significant with the X-type than with the Y-type systems. This result is consistent with the well-established fact (*19*) that Y-type zeolites are generally more

TABLE 1

Si/Al Ratios and the Extents of Dealumination (%) of the X and Y Zeolites Treated with 1 *N* Cation Chloride Solutions

Ion	pK_h[a]	13X			SK40		
		pH	Si/Al	$-\Delta$Al(%)[b]	pH	Si/Al	$-\Delta$Al(%)[b]
Na^+	14.48	8.84	1.03	0.00	8.52	2.55	0.00
K^+	—	8.41	1.04	0.96	8.16	2.55	0.00
Ca^{2+}	12.70	6.62	1.09	5.50	6.52	2.55	0.00
Fe^{2+}	10.10	5.21	1.10	6.36	5.02	2.60	1.92
Co^{2+}	9.60	5.13	1.11	7.21	4.81	2.67	4.50
Cu^{2+}	7.53	3.37	1.45	29.0	3.17	2.79	8.60
Fe^{3+}	2.19	1.33	76.4	98.7	1.01	51.6	95.1
H^+	—	0.21	71.4	98.6	0.14	83.5	96.9

[a] Values of pK_h (negative log of the first hydrolysis constant of cation obtained from Yatsimirksii (*20*)).

[b] Dealumination percentage: Al amount extracted/Al amount in Na^+-zeolite.

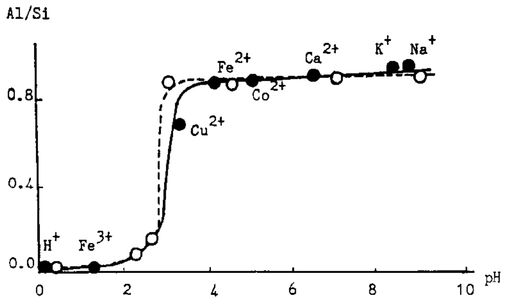

FIG. 1. Plots of the Al/Si ratio of ion-exchanged zeolite (13X) against pH. ○, Treated by HCl solution; ●, treated by 1 *N* cation chloride solution.

stable than X-type zeolites in thermal and chemical treatments.

In order to remove aluminum atoms from zeolites by chemical treatments, we treated the zeolites with 1 *N* chloride solutions containing various cations. The final acidity (pH) of the solution is correlated to the hydrolysis power or pK_h of the cation as shown in Table 1.

The extents of dealumination of the X- and Y-type zeolites are summarized in Table 1. The effect of monovalent cations, except H$^+$, on the zeolite dealumination is almost negligible as shown in Table 1. However, the solution of divalent cation causes a considerable dealumination without disturbing the crystal structure. In the cases of Fe^{3+} and H$^+$ ions, more than 90% faujasite aluminum was removed and the crystal structure was significantly destroyed. By comparison of the chemical stability of the X- and Y-type zeolites in terms of dealumination, the X type is obviously less stable than the Y type.

As shown in Figs. 1 and 2, the treatments of the X- and Y-type zeolites with varying concentrations of HCl provide the same extents of dealumination as the treatments with the cation solutions. Accordingly, it seems quite reasonable to conclude that the cation effect on the dealumination is the effect of acidity of the solution.

A schematic illustration of an initial dealumination process of zeolites by the acid treatment is shown in Scheme 1. The oxygen atom bonded to the aluminum atom is considered to be an adsorption center for protons because of its large negative charge density. This situation may not be essentially different in both the X- and the Y-type zeolites. The present dealumination mechanism is essentially identical with that proposed very recently by Lee and Rees (*21*).

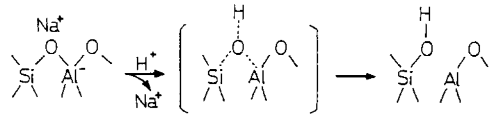

SCHEME 1

In order to obtain more specific qualitative information for the above dealumination mechanism, we made CNDO/2 calculations on a model of the sixfold cluster, $T_6O_6(OH)_{12}$ in Fig. 3, which simulates the $S_{I'}$ and S_{II} sites of faujasite zeolite. The atoms T_1, O_2, T_3, T_5, O_6, T_7, T_9, O_{10}, and O_{11} are all in the same plane, whereas the atoms O_4, O_8, and O_{12} are slightly lifted over the plane with the dihedral angle of 30°. This arrangement produces a minimum energy state.

For an X-type zeolite whose Si/Al ratio is 1, T_3, T_7, and T_{11} positions are occupied by Al atoms. On the other hand, a Y-type zeolite (Si/Al = 2.55) consists of a mixture of $Al_2Si_4O_6(OH)_{12}$ (T_3 and T_9; Al) and $AlSi_5O_6(OH)_{12}$ (T_3; Al).

Table 2 lists the charge densities of each skeletal atom of the cluster. The oxygens are considered to be the reaction sites for dealumination because of the negative

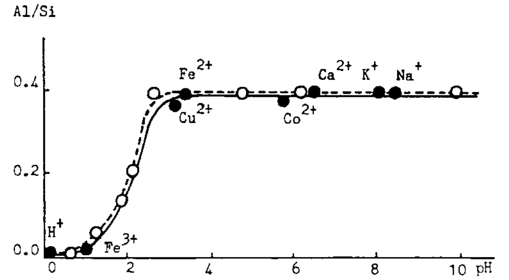

FIG. 2. Plots of the Al/Si ratio of ion-exchanged zeolite (SK40) against pH. ○, Treated by HCl solution; ●, treated by 1 *N* cation chloride solution.

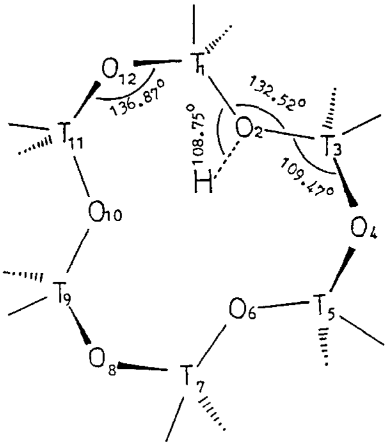

FIG. 3. Schematic depiction of cluster model of cationic sites ($S_{I'}$, S_{II}). For Si/Al = 1, T_3, T_7, and T_{11} are Al atoms; Si/Al = 2, T_3 and T_9 are Al atoms; Si/Al = 5, T_3 is an Al atom.

charges on them. Beran (*12*) suggested that hydroxyl groups are formed on the position of the oxygen atoms bonded to Al. These hydroxyl groups have been experimentally demonstrated to exist in real zeolite crystals (*22*). When the cation is placed on the sites, $S_{I'}$ or S_{II}, it is attracted to the most negatively charged aluminum oxygen, O_2 in Fig. 3. The distance between the cation and O_2 is determined by both the cation size and the interaction strength between the cation and other oxygen atoms. The equilibrium bond lengths of Na^+–O_2 and H^+–O_2 were calculated to be 0.231 and 0.103 nm, respectively.

TABLE 2

CNDO/2 Charge Densities (q) for the Cluster Model $T_6O_6(OH)_{12}$ with Various Si/Al Ratios

c.d.	Si/Al			
	1	2	5	∞
q_1	1.4490	1.5314	1.5580	1.6584
q_2	−0.7147	−0.7226	−0.7327	−0.7519
q_3	1.3137	1.3237	1.3594	1.6584
q_4	−0.7224	−0.7035	−0.6836	−0.7227
q_5	1.4490	1.5294	1.5462	1.6584
q_6	−0.7147	−0.6765	−0.7076	−0.7519
q_7	1.3137	1.5268	1.6283	1.6584
q_8	−0.7224	−0.7034	−0.7354	−0.7227
q_9	1.4490	1.3371	1.6396	1.6584
q_{10}	−0.7147	−0.6844	−0.7237	−0.7519
q_{11}	1.3137	1.5343	1.6322	1.6584
q_{12}	−0.7224	−0.7013	−0.7448	−0.7227

TABLE 3

CNDO/2 Wiberg Bond Orders (P) for the Clusters $T_6O_6(OH)_{12}$, Na^+–$T_6O_6(OH)_{12}$, and H^+–$T_6O_6(OH)_{12}$ with Si/Al = 1

b.o.	Cluster		
	$T_6O_6(OH)_{12}$	Na^+–$T_6O_6(OH)_{12}$	H^+–$T_6O_6(OH)_{12}$
$P_{1\text{-}2}$	0.9682	0.9068	0.5530
$P_{2\text{-}3}$	0.6457	0.6001	0.3616
$P_{3\text{-}4}$	0.6472	0.5951	0.7742
$P_{4\text{-}5}$	0.9877	0.9246	0.9030
$P_{5\text{-}6}$	0.9682	0.9200	0.9896
$P_{6\text{-}7}$	0.6457	0.6034	0.5989
$P_{7\text{-}8}$	0.6472	0.5977	0.6376
$P_{8\text{-}9}$	0.9877	0.9284	0.9905
$P_{9\text{-}10}$	0.9682	0.9182	0.9170
$P_{10\text{-}11}$	0.6457	0.6076	0.7089
$P_{11\text{-}12}$	0.6472	0.5876	0.4949
$P_{1\text{-}12}$	0.9877	0.9265	1.0862

The calculated CNDO/2 Wiberg bond orders (P) of the clusters $T_6O_6(OH)_{12}$, Na^+–$T_6O_6(OH)_{12}$, and H^+–$T_6O_6(OH)_{12}$ for the X-type zeolite whose Si/Al ratio is 1 are summarized in Table 3.

When a Na^+ ion is added on the adsorption site, $S_{I'}$ or S_{II}, most of the bond orders of T–O are slightly reduced compared to those for the cluster without the cation.

TABLE 4

CNDO/2 Wiberg Bond Orders (P) for the Clusters, $T_6O_6(OH)_{12}$, Na^+–$T_6O_6(OH)_{12}$, and H^+–$T_6O_6(OH)_{12}$ with Si/Al = 2

b.o.	Cluster		
	$T_6O_6(OH)_{12}$	Na^+–$T_6O_6(OH)_{12}$	H^+–$T_6O_6(OH)_{12}$
$P_{1\text{-}2}$	1.0119	0.9163	0.5725
$P_{2\text{-}3}$	0.6112	0.5479	0.3434
$P_{3\text{-}4}$	0.6094	0.5654	0.7321
$P_{4\text{-}5}$	1.0202	0.9459	0.9515
$P_{5\text{-}6}$	0.8254	0.7830	0.8350
$P_{6\text{-}7}$	0.8241	0.7813	0.7703
$P_{7\text{-}8}$	1.0222	0.9488	1.0175
$P_{8\text{-}9}$	0.6047	0.5623	0.6195
$P_{9\text{-}10}$	0.6166	0.5473	0.5284
$P_{10\text{-}11}$	1.0262	0.9234	1.0417
$P_{11\text{-}12}$	0.8187	0.8122	0.6825
$P_{1\text{-}12}$	0.8142	0.8055	0.7919

TABLE 5

CNDO/2 Wiberg Bond Orders (*P*) for the Clusters, $T_6O_6(OH)_{12}$, Na^+–$T_6O_6(OH)_{12}$, and H^+–$T_6O_6(OH)_{12}$ with Si/Al = 5

b.o.	Cluster		
	$T_6O_6(OH)_{12}$	Na^+–$T_6O_6(OH)_{12}$	H^+–$T_6O_6(OH)_{12}$
$P_{1\text{-}2}$	1.0828	0.9667	0.5813
$P_{2\text{-}3}$	0.5878	0.5228	0.3288
$P_{3\text{-}4}$	0.5878	0.5477	0.6970
$P_{4\text{-}5}$	1.0528	0.9862	0.9862
$P_{5\text{-}6}$	0.7300	0.6780	0.7407
$P_{6\text{-}7}$	0.9107	0.8441	0.8712
$P_{7\text{-}8}$	0.8077	0.7759	0.7948
$P_{8\text{-}9}$	0.8600	0.8259	0.8813
$P_{9\text{-}10}$	0.8555	0.7926	0.7705
$P_{10\text{-}11}$	0.8109	0.7592	0.8578
$P_{11\text{-}12}$	0.9134	0.8635	0.7665
$P_{1\text{-}12}$	0.7331	0.7035	0.9157

Nevertheless, upon replacement of H^+ for Na^+, the bond weakening becomes more significant. The bond order of the O_2–Al bond, in particular, becomes about one-half of the original $P_{2\text{-}3}$. The reduced bond order facilitates Al–O bond cleavages. Similar weakenings of the Al–O bond are also found for the Y-type zeolite as shown in Tables 4 and 5. Such bond weakenings suggest the dealumination reaction mechanism illustrated in Scheme 2.

The terminal OH (in the state IV) was rotated around the Si–O axis to obtain a minimum bond order $P_{2\text{-}3}$ and the most stable energy state without disturbing the hexagonal structure. The most probable dihedral angles of the Si–O axis are found to be −19° and −18° for the X- and Y-type zeolites, respectively, as shown in Table 6. The O_2–H bond exhibits spatial arrangements of 8° of dihedral angle with respect to the cluster plane for the X-type zeolite and the corresponding angle 11°–12° for the Y-type zeolite.

TABLE 6

Total Energy (E_i) as a Function of Dihedral Angles (ϕ) of the Bonds T_1–O_2 and O_2–H Toward the Main Plane

Bond	Si/Al					
	1		2		5	
	ϕ (°)	E_1	ϕ (°)	E_2	ϕ (°)	E_5
T_1–O_2	−17	−350.4096	−17	−352.2498	−17	−353.9921
	−18	−350.4123	−18	−352.2605	−18	−353.9994
	−19	−350.4195	−19	−352.2534	−19	−353.9936
	−20	−350.4135	−20	−352.2434	−20	−353.9908
O_2–H	7	−350.4221	10	−352.2613	11	−353.9992
	8	−350.4237	11	−352.2621	12	−353.9994
	9	−350.4214	12	−352.2605	13	−353.9936

TABLE 7

CNDO/2 Charge Densities (*q*) for the Cluster Models with Various Si/Al Ratios after Breaking of an Al–O Bond

c.d.	Si/Al		
	1	2	5
q_1	1.5290	1.6488	1.6720
q_2	−0.5095	−0.5163	−0.5239
q_3	1.2829	1.2919	1.2871
q_4	−0.7357	−0.7637	−0.7639
q_5	1.5100	1.5835	1.5999
q_6	−0.7205	−0.6778	−0.6781
q_7	1.3310	1.5457	1.6496
q_8	−0.7273	−0.6847	−0.7228
q_9	1.4878	1.3501	1.6562
q_{10}	−0.7144	−0.7055	−0.7510
q_{11}	1.3276	1.5552	1.6586
q_{12}	−0.6980	−0.7301	−0.7240

The enhanced charge density (q_4) on O_4 oxygen atom in Table 7 indicates that the

TABLE 8

CNDO/2 Wiberg Bond Orders (*P*) for Cluster Models (State V) with Various Si/Al Ratios

b.o.	Si/Al		
	1	2	3
$P_{1\text{-}2}$	0.7017	0.7272	0.7342
$P_{3\text{-}4}$	0.4686	0.4365	0.4103
$P_{4\text{-}5}$	0.4819	0.5097	0.5339
$P_{5\text{-}6}$	1.1108	1.0463	0.9855
$P_{6\text{-}7}$	0.5062	0.5795	0.6689
$P_{7\text{-}8}$	0.7636	1.0767	0.9072
$P_{8\text{-}9}$	0.9162	0.5089	0.7756
$P_{9\text{-}10}$	0.9545	0.5829	0.8258
$P_{10\text{-}11}$	0.6508	1.0090	0.8021
$P_{11\text{-}12}$	0.5306	0.7165	0.8090
$P_{1\text{-}12}$	1.0757	0.9529	0.8735

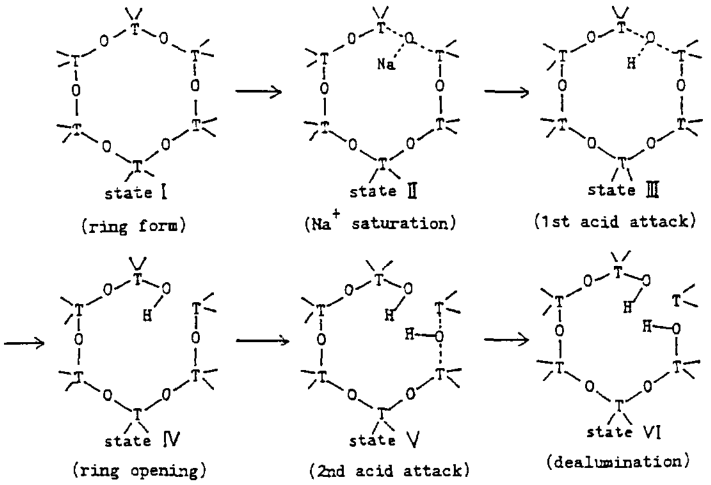

SCHEME 2

most probable site for the second acid attack is O_4 for the completion of the dealumination process. Bond weakenings due to the second attack are significant as shown by the bond orders $P_{3\text{-}4}$ in Table 8.

The total energies for the clusters in each reaction step are computed by CNDO/2 and listed in Table 9. The proposed reaction mechanism from state I to state VI seems reasonable, for the total energy decreases in each step regardless of the Si/Al ratio. The ΔE value for the X-type zeolite decrease more than those for the Y-type zeolite. The proton donations toward negatively charged oxygen sites, in state III and state V, are highly probable as deduced from the stabilization energies, ΔE_1, ΔE_2, and ΔE_5. Taking into account the energy difference, we suggest that the second proton donation in state V takes place more readily than the first one. The equilibrium constant (K) computed from ΔE for the X-type zeolite is always three to five times larger than that for the Y-type zeolite (if the reaction temperature is held constant). These results support the claim that X-type zeolites are chemically more unstable than the Y-type zeolites in the dealumination reaction. Accordingly, it seems reasonable to conclude that for the dealumination during ion-exchange procedures the cation effect may be just another version of the acidity effect. The theoretical calculations suggest that acid attacks are performed at the oxy-

TABLE 9

Total Energies for the Clusters at Each Reaction State

Cluster	Si/Al, ΔE					
	1	ΔE_1[a]	2	ΔE_2[a]	5	ΔE_5[a]
State I	−349.0304	—	−350.9924	—	−352.8944	—
State II	−349.4525	0.4221	−351.2874	0.2950	−353.0041	0.1097
State III	−349.9730	0.5205	−351.8422	0.5548	−353.6041	0.6000
State IV	−350.4237	0.4507	−352.2621	0.4199	−353.9994	0.3953
State V	−351.1795	0.7558	−352.8924	0.6303	−354.5303	0.5309
State VI	−351.4239	0.2404	−353.0860	0.1936	−354.7190	0.1887

[a] ΔE_1, ΔE_2, and ΔE_5 stand for the energy difference between the state and the former state.

gen sites which are attached to the aluminum atoms of the framework. The experimental findings that the dealumination of the X-type zeolite occurs more readily than that of the Y-type zeolite are rationalized by the results achieved in the CNDO/2 calculation, assuming the acid attack mechanism.

REFERENCES

1. Barthomeuf, D., *J. Phys. Chem.* **83,** 249 (1979).
2. Bosacek, V., Patzelova, V., Tvaruzkova, Z., Freude, D., Lohse, U., Schirmer, W., Stach, H., and Thamm, H., *J. Catal.* **61,** 435 (1980).
3. Kerr, G. T., *J. Phys. Chem.* **72,** 2594 (1968).
4. Barthomeuf, D., and Beaumont, R., *J. Catal.* **30,** 288 (1973).
5. Barthomeuf, D., and Beaumont, R., *J. Catal.* **27,** 45 (1972).
6. Decanio, S. J., Sohn, J. R., Fritz, P. O., and Lunsford, J. H., *J. Catal.* **101,** 132 (1986).
7. Beaumont, R., and Barthomeuf, D., *J. Catal.* **26,** 218 (1972).
8. Beagley, B., Dwyer, J., Fitch, F. R., Mann, R., and Walter, J., *J. Phys. Chem.* **88,** 1744 (1984).
9. Dempsey, E., *J. Phys. Chem.* **73,** 3660 (1969).
10. Beran, S., Jiru, P., and Wichterlova, *J. Phys. Chem.* **85,** 1951 (1981).
11. Melchoir, M. T., Vaughan, D. E. W., and Jacobson, A. J., *J. Amer. Chem. Soc.* **104,** 4859 (1982).
12. Beran, S., *J. Phys. Chem.* **89,** 5589 (1985).
13. Beran, S., *J. Phys. Chem. Solids* **43,** 221 (1982).
14. Olson, D. H., *J. Phys. Chem.* **74,** 2758 (1970).
15. Shannon, R. D., and Prewitt, C. T., *Acta Crystallogr. Sect. B* **25,** 925 (1969).
16. Mortier, W. J., and Geerlings, P., *J. Phys. Chem.* **84,** 1982 (1980).
17. Beran, S., and Dubsky, J., *J. Phys. Chem.* **83,** 2538 (1979).
18. Pople, J. A., Santry, D. P., and Segal, G. A., *J. Phys. Chem.* **43,** S129 (1965).
19. Kladning, W., *J. Phys. Chem.* **80,** 262 (1976).
20. Yatsimirskii, K. B., "Instability Constant of Complex Compounds." Pergamon, Elmsford, NY (1960).
21. Lee and Rees, *J. Chem. Soc. Faraday. Trans. I* **83,** 1531 (1987).
22. Heo, N. H., Cruz-Patalinghug, W., and Seff, K., *J. Phys. Chem.* **90,** 3931 (1986).